Activation Loop Dynamics are Coupled to Core Motions in Extracellular-signal Regulated Kinase-2

Dylan B. Iverson[¶], Yao Xiao[¶], David N. Jones[‡], Elan Z. Eisenmesser[§] and Natalie G. Ahn[¶]

[¶]Department of Biochemistry, University of Colorado at Boulder, Boulder, CO 80309;
[‡]Department of Pharmacology and [§]Department of Biochemistry and Molecular Genetics, University of Colorado Denver Anschutz Medical Campus, Aurora, CO 80045

SUPPORTING INFORMATION

1. Detailed Materials and Methods

2. Figures S1-S6

3. Tables S1-S3

1. Detailed Materials and Methods

Protein Preparations.

[*methyl*-^{13}C]ILV-labeled ERK2 was generated as described (Turaginov & Kay, 2003) and applied to ERK2 as described (Xiao et al., 2014, 2015). BL21(DE3) pLysS chemically competent *E. coli* was transformed with the plasmid pET23a containing rat His_6-ERK2 (Xiao et al., 2014). Recombinant *E. coli* was grown at 37ºC with shaking in 1 L of D_2O-based M9 salt minimal medium containing 3 g D-glucose-d_7, 1 g $^{15}NH_4Cl$, and vitamins and trace minerals. At OD(600 nm) ≈ 0.8, 2-keto-3-(methyl-d_3)-butyric acid-4-^{13}C,3-d_1 and 2-ketobutyric acid-4-^{13}C,3,3-d_2 were added to final concentrations of 0.7 mM and 0.4 mM, respectively. Growth was allowed to proceed for 1 h longer, after which cultures were chilled for 10 min. Protein was induced by addition of 160 μM IPTG and allowed to express at 18ºC with shaking for 16 h. (The low temperature during protein expression helps minimize autophosphorylation.) Cells were harvested by centrifugation and pellets were stored frozen at -20ºC. For protein purification, cell pellets were resuspended in lysis buffer (50 mM sodium phosphate, pH 8.0, 300 mM NaCl, 0.1% (v/v) 2-mercaptoethanol, 5 mM imidazole, 1×cOmplete protease inhibitor (Roche), 1 mg/mL lysozyme, and 1 mM EDTA). Cells were mixed gently at room temperature for 20 min, sonicated, and centrifuged at 15,000 rpm, 4ºC for 45 min. ERK2 was purified from the supernatant by Ni^{2+}-NTA (Bio-Rad) affinity chromatography (buffer: 50 mM sodium phosphate, pH 8.0, 300 mM NaCl, 0.1% (v/v) 2-mercaptoethanol, 5-300 mM imidazole). Afterwards, 10,000 MW cutoff centrifugal spin filters were used to exchange buffer prior to purification by HiTrap Q HP (GE Healthcare) anion exchange FPLC (buffer: 50 mM Tris, pH 7.4, 2.5% (v/v) glycerol, 5 mM $MgSO_4$, 5 mM DTT, 0-1 M NaCl), and then again to concentrate protein prior to Superdex 200 10/300 GL (GE Healthcare) size exclusion FPLC (buffer: 50 mM Tris, pH 7.4, 150 mM NaCl, 5 mM $MgSO_4$, 0.1 mM EDTA, 5 mM DTT, 2.5% (v/v) glycerol, 10% D_2O). Activated dual phosphorylated ERK2 (2P-ERK2) was generated using constitutively active mutant MKK1-G7B(ΔN4/S218D/S222D) as described (Mansour et al., 1996; Shapiro et al., 1998), followed again by purification *via* HiTrap Q HP and Superdex 200 FPLC. For NMR studies, [*methyl*-^{13}C]-labeled 0P-ERK2 and 2P-ERK2 proteins were concentrated using centrifugal spin filters to 0.3–0.4 mM and exchanged into NMR buffer (50 mM Tris, pH 7.4, 150 mM NaCl, 5 mM $MgSO_4$, 0.1 mM EDTA, 5 mM DTT, 2.5% (v/v) glycerol in D_2O). The ERK2 mutants L182A, L182I, V186A, V186I and $M_{106}G/E_{107}G$ ("ME/GG") were constructed by site-directed mutagenesis of the pET23a plasmid bearing rat His_6-ERK2 and protein samples generated as above.

2D NMR Experiments and ILV-Methyl Side-Chain Assignments.

NMR data were collected at 25ºC using a Varian 900 MHz Direct Drive NMR system with z-axis cryoprobe and processed with NMRPipe software package (Delaglio et al., 1995). 2D (^{13}C,^{1}H) methyl transverse relaxation-optimized spectroscopy (TROSY) HMQC spectra were collected for 4 mutants (L182A, L182I, V186A, and V186I) of ERK2 in their 0P and 2P forms. Many peaks in the spectrum of wild-type 0P- and 2P-ERK2 were previously assigned as described (Xiao et al., 2015). Two residues, Leu182 and Val186, were previously unassigned but important probes to monitor activation loop dynamics. Therefore, 2D (^{13}C,^{1}H) HMQC spectra of mutants in 0P-ERK2 and 2P-ERK2 (0.3-0.4 mM) were generated to assign these residues by observing peak disappearances. Where possible, peak assignments were verified by use of through-space (under 9 Å) interactions detected in 3D (^{13}C,^{13}C,^{1}H) HMQC-NOESY spectra.

3D (^{13}C, ^{13}C, ^{1}H) HMQC-NOESY experiments were collected using non-uniform sampling methods (Barna et al., 1987) using the Poisson-gap sampling schemes implemented by Hyberts et al. (2010) with a sampling density of 50%. Data were processed using the istHMS package v2111 (Hyberts et al., 2012, 2014) in combination with NMRPipe (Delaglio et al, 1995) and analyzed

using CCPNMR Analysis v 2.4.2 (Vranken et al., 2005). Experiments were performed on the [*methyl*-^{13}C]ILV labeled samples of 0P-ERK2 and 2P-ERK2, using a 350 ms mixing time. The experiments on 0P-ERK2 were acquired with 54 and 52 complex points (15.9 and 15.3 ms, respectively) in the t_1 (^{13}C) and t_2 (^{13}C) dimensions, and 1024 complex points in the acquisition period. GARP1 ^{13}C decoupling was applied during the 73 ms acquisition period (Palmer, 2004). A 1.8 s delay period was used with 8 scans, leading to a total acquisition time of 56 h. The NOESY experiments for 2P-ERK2 were essentially the same, except that 64 and 64 complex points were used (18.8 and 18.8 ms, respectively) in the t_1 (^{13}C) and t_2 (^{13}C) dimensions, resulting in a total acquisition time of 82 h. Time-domain data in the ^{1}H dimension were apodized by a squared cosine window function and zero-filled prior to Fourier transformation. The number of points in both indirect dimensions was doubled using forward-backward linear prediction (Zhu & Bax, 1992). The indirect dimensions were then apodized by a cosine window function and zero-filled prior to Fourier transformation and baseline corrections were applied to both indirect dimensions.

References

Barna JCJ, Laue ED, Mayger MR, Skilling J, Worrall SJP (1987) Exponential sampling, an alternative method for sampling in two-dimensional NMR experiments. *J Magn Reson* 73:69-77.

Delaglio F, Grzesiek S, Vuister GW, Zhu G, Pfeifer J, Bax A (1995) NMRPipe: A multidimensional spectral processing system based on UNIX pipes. *J Biomol NMR* 6:277-293.

Hyberts SG, Takeuchi K, Wagner G (2010) Poisson-gap sampling and forward maximum entropy reconstruction for enhancing the resolution and sensitivity of protein NMR data. *J Am Chem Soc* 132:2145-2147.

Hyberts SG, Milbradt AG, Wagner AB, Arthanari H, Wagner G (2012) Application of iterative soft thresholding for fast reconstruction of NMR data non-uniformly sampled with multidimensional Poisson Gap scheduling. *J Biomol NMR* 52:315-327.

Hyberts SG, Arthanari H, Robson SA, Wagner G (2014) Perspectives in magnetic resonance: NMR in the post-FFT era. *J Magn Reson* 241:60-73.

Mansour SJ, Candia JM, Matsuura JE, Manning MC, Ahn NG (1996) Interdependent domains controlling the enzymatic activity of mitogen-activated protein kinase kinase 1. *Biochemistry* 35:15529-15536.

Palmer AG (2004) NMR characterization of the dynamics of biomacromolecules. *Chem Rev* 104:3623-3640.

Shapiro PS, Vaisberg E, Hunt AJ, Tolwinski NS, Whalen AM, McInsoth JR, Ahn NG (1998) Activation of the MKK/ERK pathway during somatic cell mitosis: direct interactions of active ERK with kinetochores and regulation of the mitotic 3F3/2 phosphoantigen. *J Cell Biol* 142:1533-1545.

Tugarinov V, Kay LE (2003) Ile, Leu, and Val methyl assignments of the 723-residue malate synthase G using a new labeling strategy and novel NMR methods. *J Am Chem Soc* 125:13868-13878.

Xiao Y, Lee T, Latham MP, Warner LR, Tanimoto A, Pardi A, Ahn NG (2014) Phosphorylation releases constraints to domain motion in ERK2. *Proc Natl Acad Sci USA* 111:2506-2511.

Xiao Y, Warner LR, Latham MP, Ahn NG, Pardi A (2015) Structure-based assignment of Ile, Leu and Val methyl groups in the active and inactive forms of the mitogen-activated kinase extracellular signal-regulated kinase 2. *Biochemistry* 54:4307-4319.

Zhu GA, Bax A (1992) 2-Dimensional linear prediction for signals truncated in both dimensions. *J Magn Reson* 98:192-199.

Figure S1

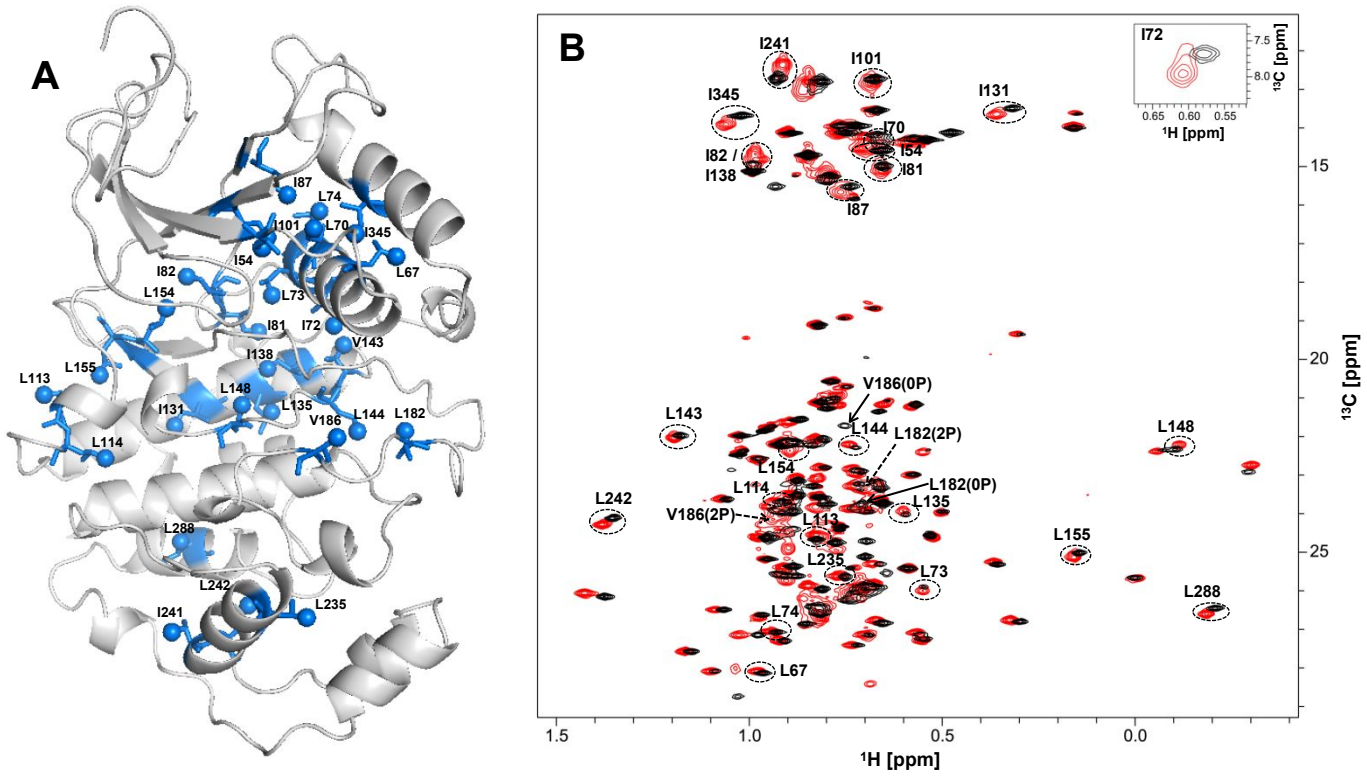

Figure S1. Residues that participate in the global conformational exchange process are distributed throughout the kinase core. (A) Residues examined in this study are shown as blue spheres in the crystal structure of 2P-ERK2 (PDBID: 2ERK). **(B)** Overlay of the full 2D [^{13}C, ^{1}H] TROSY HMQC spectra for 0P-ERK2 (black) and 2P-ERK2 (red). The resonances corresponding to residues in panel A are labeled. Arrows point to resonances of L182 and V186, whose chemical shifts change dramatically between 0P-ERK2 and 2P-ERK2. L182 and V186 are adjacent to phosphorylated residues T183 and Y185, respectively, and are used in this study to report activation loop motions.

Figure S2

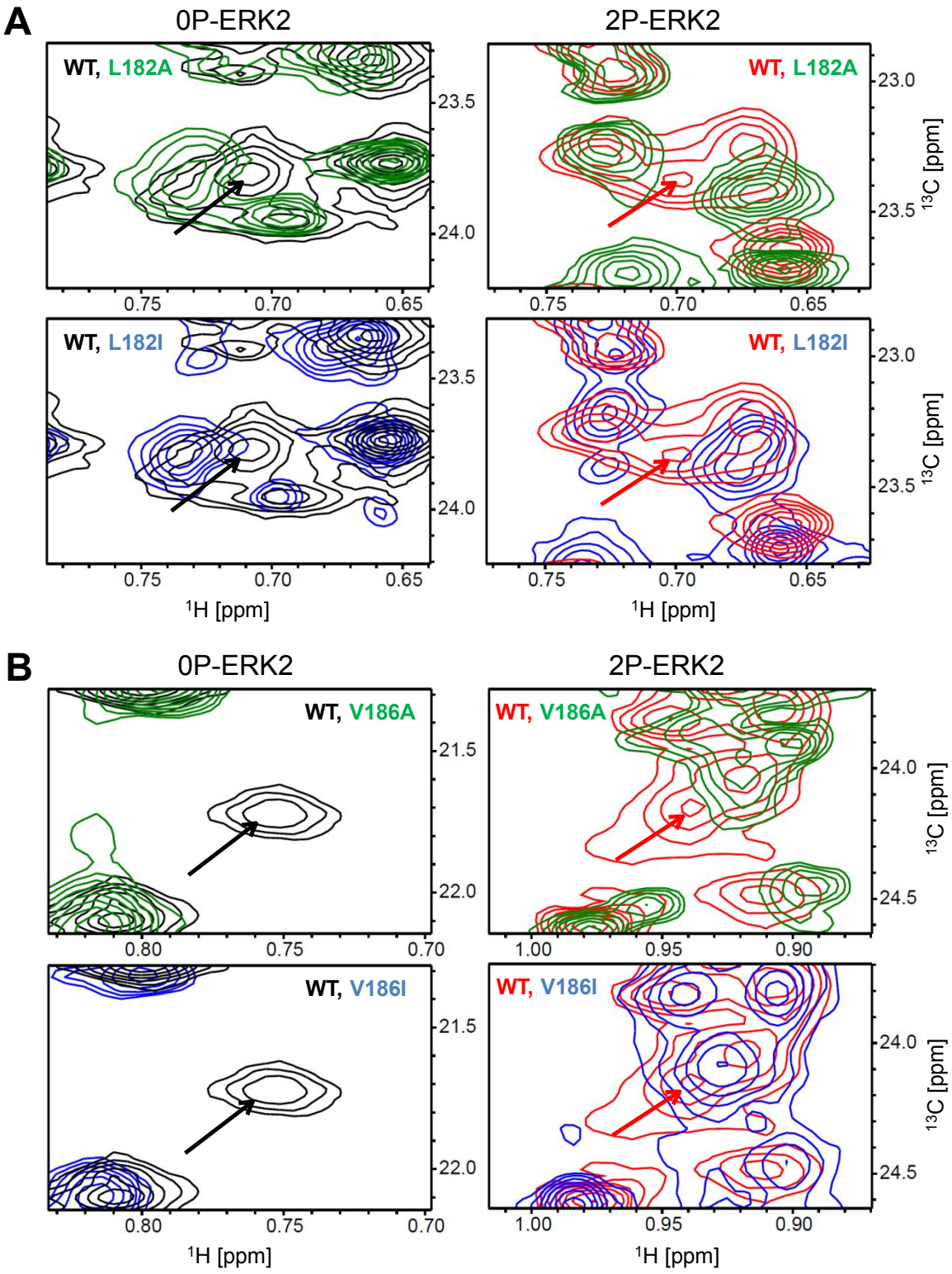

Figure S2. Assignments of NMR resonances for activation loop residues L182 and V186. Activation loop residues were assigned by site-directed mutagenesis of **(A)** L182 to yield mutants L182A and L182I, and **(B)** V186 to mutants V186A and V186I. 2D [^{13}C,^{1}H] TROSY HMQC spectra of WT 0P-ERK2 (black) and 2P-ERK2 (red) are overlaid with spectra of mutants in corresponding phosphorylation states. Resonances were identified from their consistent peak disappearances in spectra of Ala mutants (green), and Ile mutants (blue) compared to WT ERK2 (indicated by arrows).

Figure S3

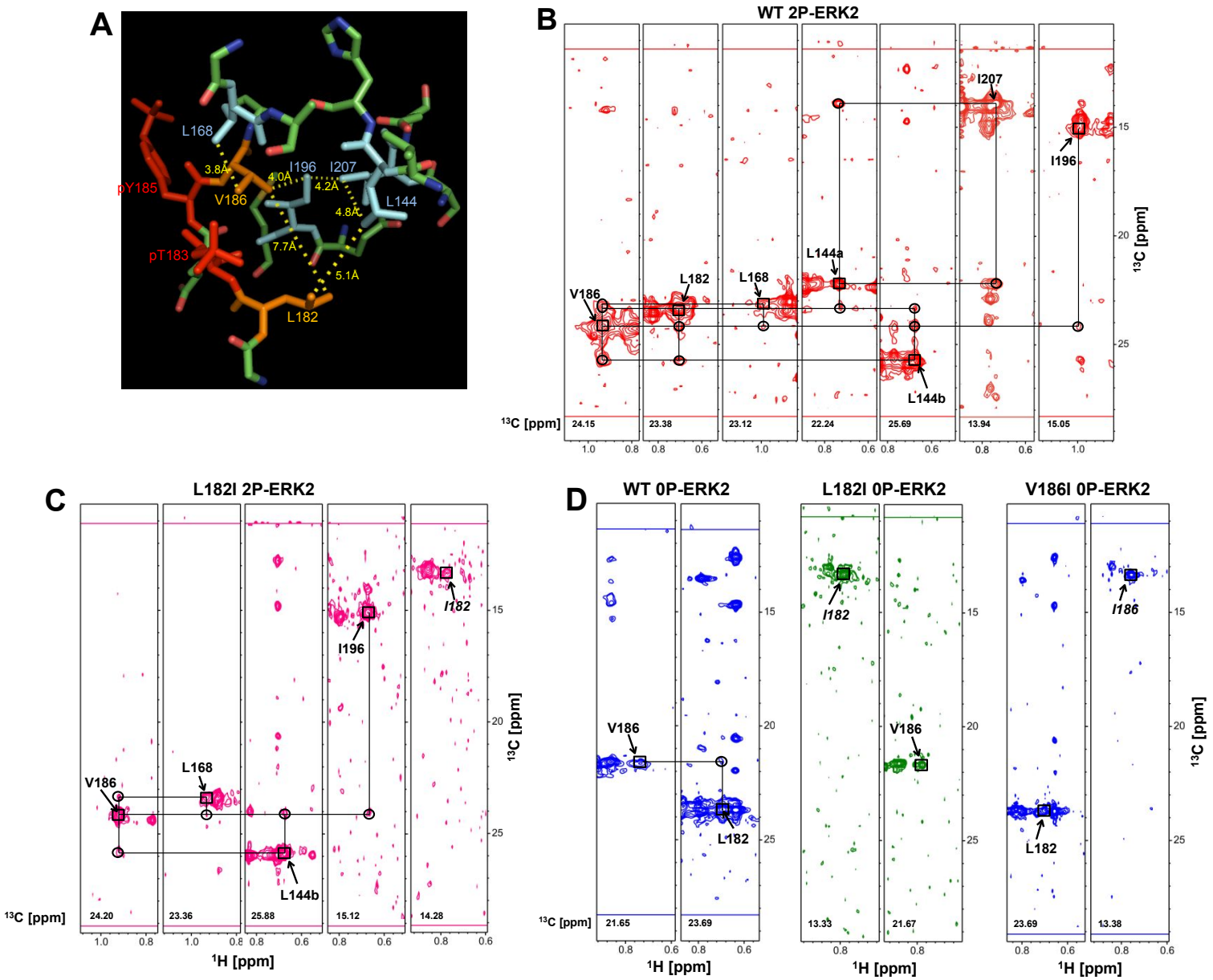

Figure S3. Activation loop residue assignments in 2P-ERK2 are confirmed by NOE through-space interactions. (A) Inter-methyl distances in the crystal structure of 2P-ERK2 (PDBID:2ERK) showing ILV methyls in proximity to activation loop residues L182 and V186, and forming a 6-residue cluster between L144, L168, L182, V186, I196, and I207. **(B)** Strip plots [^{13}C, ^{1}H] from the 3D (^{13}C,^{13}C, ^{1}H) HMQC-NOESY spectrum of 2P-ERK2 illustrate expected interactions shown in panel A. The chemical shifts (ppm) of the ^{13}C dimension are labeled at the bottom of each strip. Labels with arrows indicate self-peaks. Cross-peaks used in assignments are indicated by ovals and associated cross-peaks and self-peaks are connected by lines. **(C)** Mutant L182I 2P-ERK2 shows similar interactions between V186 and surrounding residues. NOE signals reporting L182 are absent, as expected of the mutant. A peak assigned to I182 shows no NOE cross-peaks, possibly due to peak broadening. In corresponding NOESY data on mutant V186I 2P-ERK2, no peak could be assigned to L182, possibly due to peak broadening (data not shown). **(D)** Strip plots of unphosphorylated (0P) variants of WT, L182I, and V186I presented as in panel B. NOE interactions are absent, except for a possible crosspeak between L182 and V186. The lack of discernable NOE interactions may by caused by increased dynamics of the activation loop in solution relative to the X-ray structure of 0P-ERK2.

Figure S4

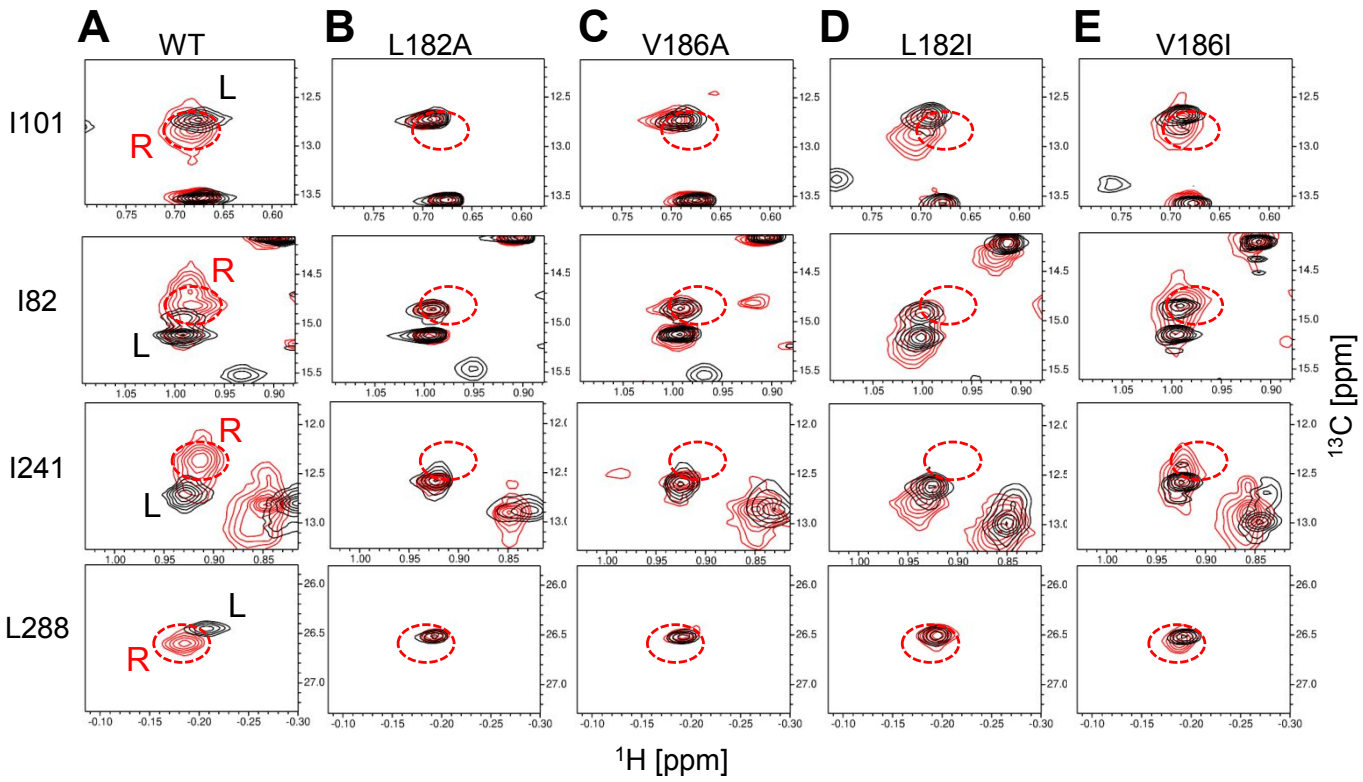

Figure S4. Methyl peaks reveal changes in conformational exchange of core residues by activation loop mutations. Shown are additional examples of two-dimensional HMQC spectra of methyl peaks in 0P-ERK2 (black) and 2P-ERK2 for representative core residues that report global motions following phosphorylation. **(A)** Peaks in WT 0P-ERK2 correspond to one conformer state ("L"), while 2P-ERK2 shifts to a new state ("R") in equilibrium with the L state (L:R ratio ≈ 20:80). **(B,C)** Activation loop mutations (**B**) L182A and (**C**) V186A disrupt the shift to the R state in 2P-ERK2. **(D,E)** More conservative activation loop mutations (**D**) L182I and (**E**) V186I mostly preserve the shift to the R state, although some residues can be observed to vary in L182I.

Figure S5

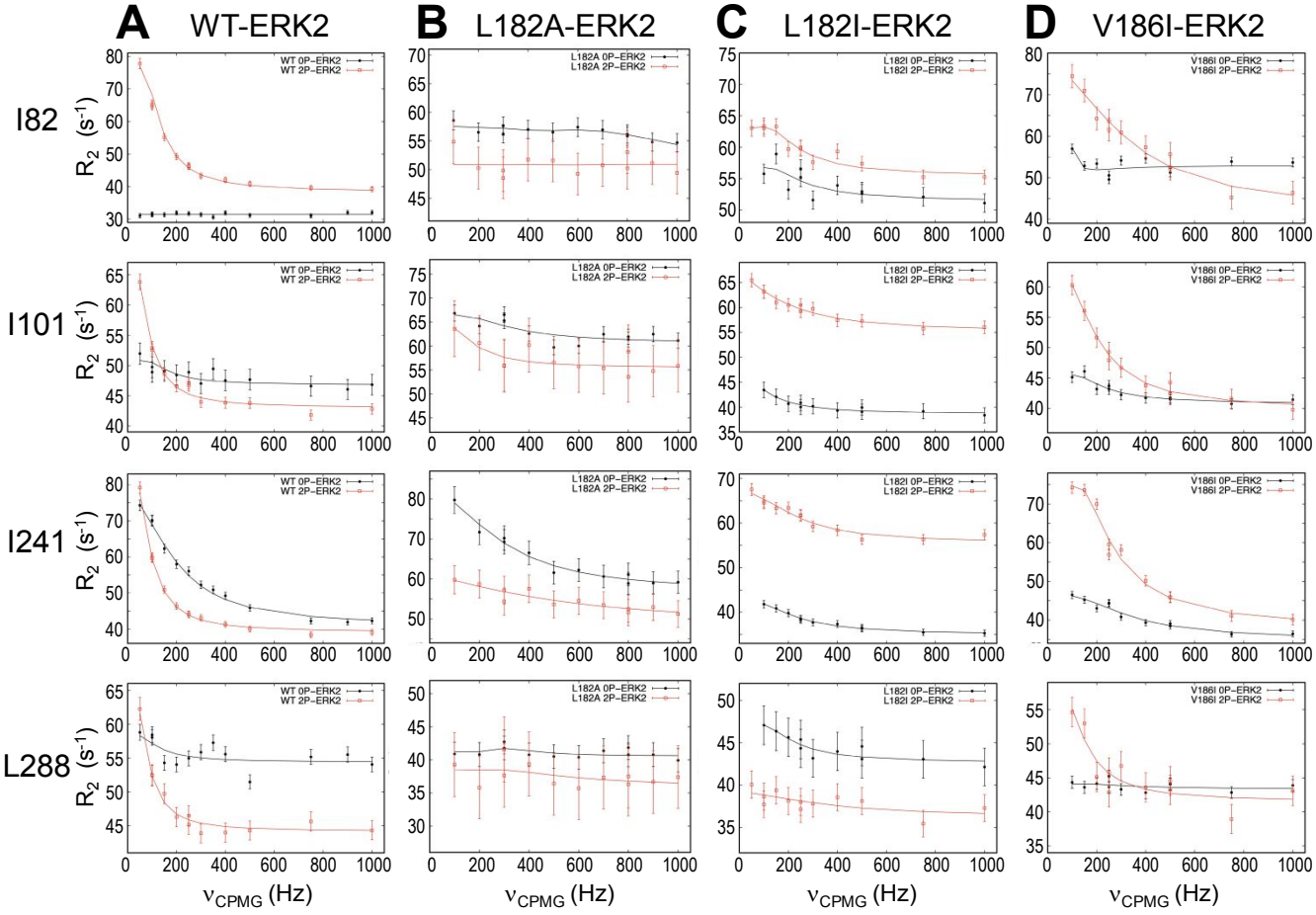

Figure S5. CPMG relaxation-dispersion plots report changes in conformational exchange of core residues by activation loop mutations. Shown are additional examples of CPMG relaxation-dispersion (RD) plots of data collected at 900 MHz for 0P-ERK2 (black) and 2P-ERK2 (red). **(A,B)** Changes in dynamics of core residues seen in (A) WT ERK2 following phosphorylation appear (B) fully blocked by mutation L182A. **(C,D)** Dynamics are (**C**) partially blocked in L182I and (**D**) unchanged in V186I. The results reveal coupling between motions of residues in the activation loop and kinase core.

Figure S6

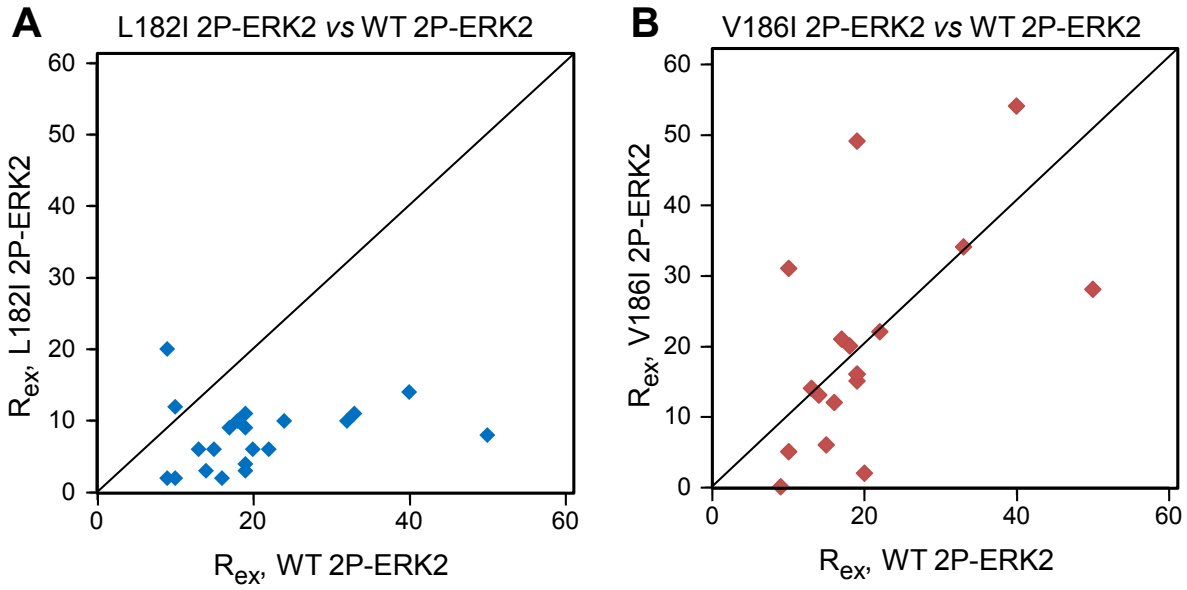

Figure S6. Suppression of R_{ex} by mutation L182I in 2P-ERK2. Plots of R_{ex} for individual residues in 2P-ERK2, comparing WT against **(A)** L182I and **(B)** V186I. R_{ex} data are listed in Supporting Information, Tables S1 and S3A,B.

Table S1. Exchange parameters for [*methyl*-^{13}C]ILV probes in WT 0P- and 2P-ERK2. [a]

	WT 0P-ERK2			WT 2P-ERK2		
	k_{ex} (s^{-1}) [b]	p_B (%) [b]	R_{ex}(s^{-1}) [c]	k_{ex} (s^{-1}) [b]	p_B (%) [b]	R_{ex}(s^{-1}) [c]
L67	ND [d]	ND	0	500 ± 280	1.8 ± 0.38	9
I70	110 ± 150	5.0 ± 6.4	4	110 ± 76	7.1 ± 3.1	15
I72	1300 ± 250	21 ± 90	24	140 ± 52	27 ± 7.7	40
L73	2400 ± 1400	6.4 ± 55	8	390 ± 92	16 ± 8.1	19
L74	ND	ND	0	92 ± 110	15 ± 10	10
I81	1800 ± 460	27 ± 42	9	410 ± 28	37 ± 22	19
I82	ND	ND	0	100 ± 33	34 ± 9.3	50
I87	2000 ± 1900	0.26 ± 0.14	1	90 ± 69	16 ± 9.2	22
I101	150 ± 160	2.8 ± 2.5	8	440 ± 30	10 ± 18	18
I131	1100 ± 200	2.9 ± 1.1	10	210 ± 43	9.9 ± 1.3	13
L135	ND	ND	9	400 ± 130	32 ± 45	24
I138	ND	ND	2	210 ± 53	17 ± 2.8	10
V143	1200 ± 370	48 ± 26	10	450 ± 47	ND	14
L148	5770 ± 16100	0.61 ± 1.1	2	470 ± 200	23 ± 78	19
L154	900 ± 480	0.97 ± 0.13	3	380 ± 240	8.3 ± 3.2	20
L155	1300 ± 680	0.69 ± 0.76	1	400 ± 97	32 ± 50	17
L182**	1600 ± 270	21 ± 97	12	72 ± 210	9.3 ± 24	6
V186**	ND	ND	0	510 ± 100	11 ± 1.8	31
I241	1200 ± 120	22. ± 30.	30	440 ± 21	17 ± 6.6	33
L288	ND	ND	2	320 ± 350	24 ± 93	16
I345	ND	ND	0	370 ± 34	22 ± 27	19
Global fit (including L182, V186)	No convergence [e]			310 ± 16	17 ± 0.44	
Global fit (w/out L182, V186)	No convergence [e]			320 ± 17	17 ± 0.45	

** [*methyl*-^{13}C] probes for activation loop residues L182 and V186

[a] Parameters were obtained from multiple quantum CPMG dispersion data collected at 25 °C.

[b] Parameters were obtained by fitting CPMG dispersion data collected at 600, 800, and 900 MHz to a two-state exchange process using the Carver-Richards equation on a per-methyl basis. The errors were estimated from fits using the CATIA program (Materials and Methods).

[c] R_{ex} was estimated using the equation $R_{ex} = R_{2,eff}(50\ \text{Hz}) - R_{2,eff}(1{,}000\ \text{Hz})$ from 900 MHz CPMG dispersion data.

[d] N.D. Individual fits and/or errors could not be determined.

[e] Global fitting attempts failed to converge.

Table S2A,B. Exchange parameters for [*methyl*-^{13}C]ILV probes in mutant ME/GG 0P-ERK2. [a]

Table S2A	ME/GG 0P-ERK2		
	k_{ex} (s^{-1}) [b]	$p_A p_B \Delta\omega_{AB}^2$ (s^{-2}) [b]	R_{ex} (s^{-1}) [c]
L54	1160 ± 186	12800 ± 1160	9
L67	2600 ± 1840	12600 ± 6400	4
I70	1440 ± 260	16200 ± 1840	8
I72	2200 ± 540	38000 ± 6600	19
I82	1200 ± 220	9200 ± 960	6
I101	2400 ± 600	26000 ± 4400	8
L113	1100 ± 380	7000 ± 1380	6
L114	1228 ± 158	14200 ± 1060	9
I131	2000 ± 640	34000 ± 7200	13
L135	1200 ± 800	12000 ± 4600	7
I138	880 ± 182	7600 ± 780	6
L144	840 ± 500	4200 ± 1220	3
L148	920 ± 380	9200 ± 1920	7
L155	2200 ± 360	20000 ± 2200	8
L182**	1780 ± 460	12400 ± 2200	6
V186**	2000 ± 620	30000 ± 6400	12
L235	1300 ± 164	30000 ± 2400	7
I241	1180 ± 58	26000 ± 760	16
L242	1380 ± 320	11800 ± 1640	6
Global fit (including L182, V186)	1300 ± 150 [d]	p_B = 10 ± 20 % [d]	
Global fit (w/out L182, V186)	1200 ± 140 [d]	p_B = 12 ± 18 % [d]	

** [*methyl*-^{13}C] probes for activation loop residues L182 and V186

[a] Parameters were obtained from multiple quantum CPMG dispersion data collected at 25 °C.

[b] This term was estimated assuming a two-state exchange model under fast-exchange limit using 900 MHz CPMG dispersion data (Materials and Methods).

[c] R_{ex} was estimated using the equation $R_{ex} = R_{2,eff}(50\ \text{Hz}) - R_{2,eff}(1{,}000\ \text{Hz})$ from 900 MHz CPMG dispersion data.

[d] Parameters were obtained by fitting CPMG dispersion data collected at 800 and 900 MHz to a two-state exchange process using the Carver-Richards equation on a per-methyl basis. The errors were estimated from fits using the CATIA program (Materials and Methods).

Table S2B Jackknife analysis [a]	ME/GG 0P-ERK2	
	k_{ex} (s^{-1}) [b]	p_B (%) [b]
Trial 1: 15 residues (4 removed)	1270 ± 57	12 ± 2.4
Trial 2: 9 residues (6 removed)	1270 ± 69	12 ± 1.9
Trial 3: 10 residues (9 removed)	1280 ± 110	11 ± 4.1
Averages:	1270 ± 79	12 ± 2.8

[a] Parameters were obtained by fitting CPMG dispersion data collected at 800 and 900 MHz, 25 °C. Each trial involved 50 iterations in which 4, 6 or 9 residues were randomly removed from the set of 19 residues shown in Table S2A. For each iteration, the remaining residues were fit to a two-state exchange process using the Carver-Richards equation on a per-methyl basis.

[b] For each trial, reported values of k_{ex} and p_B represent averages and standard deviations over 50 iterations.

Table S3A. Exchange parameters for [*methyl*-^{13}C]ILV probes in mutant L182I, 0P- and 2P-ERK2. [a]

Table S3A L182I	L182I 0P-ERK2			L182I 2P-ERK2		
	k_{ex} (s^{-1}) [b]	$p_A p_B \Delta\omega_{AB}^2$ (s^{-2}) [b]	R_{ex}(s^{-1}) [c]	k_{ex} (s^{-1}) [b]	$p_A p_B \Delta\omega_{AB}^2$ (s^{-2}) [b]	R_{ex}(s^{-1}) [c]
L67	1400 ± 510	10000 ± 1600	4	790 ± 470	4100 ± 1200	2
I70	2600 ± 900	11000 ± 2100	3	860 ± 200	6900 ± 820	6
I72	1900 ± 330	21000 ± 1900	16	1800 ± 220	31000 ± 2400	14
L73	790 ± 200	22000 ± 2000	13	1600 ± 230	20000 ± 1800	11
L74	1200 ± 510	7600 ± 1200	3	270 ± 520	1500 ± 1100	2
I81	2500 ± 610	21000 ± 2800	5	1300 ± 230	13000 ± 1300	9
I82	1900 ± 780	14000 ± 2900	4	1800 ± 280	18000 ± 1800	8
I87	4200 ± 2100	12000 ± 4000	3	1100 ± 440	8600 ± 1900	6
I101	730 ± 160	6800 ± 510	5	1300 ± 120	14000 ± 770	10
I131	810 ± 370	5100 ± 800	3	700 ± 200	5800 ± 760	5
L135	1100 ± 470	11000 ± 1800	6	1300 ± 310	16000 ± 2200	10
I138	1700 ± 340	11000 ± 1000	5	1500 ± 150	21000 ± 1300	12
V143	360 ± 260	11000 ± 5000	4	680 ± 880	1400 ± 860	3
L148	940 ± 350	11000 ± 1500	7	2100 ± 650	13000 ± 2500	4
L154	2300 ± 1300	7700 ± 2400	3	2500 ± 170	21000 ± 950	6
L155	2400 ± 670	29000 ± 4600	9	1500 ± 250	16000 ± 1600	9
I182**	1900 ± 300	31000 ± 2500	11	1300 ± 390	43000 ± 7300	20
V186**	1300 290	31000 ± 2900	17	2200 ± 360	27000 ± 2900	10
I241	1400 ± 82	14000 ± 340	7	1500 ± 170	19000 ± 1300	11
L288	1700 ± 370	11000 ± 1100	3	3100 ± 1300	10000 ± 3100	2
I345	16000 ± 46000	24000 ± 63000	0	430 ± 170	3800 ± 560	3
Global fit (including I182, V186)	690 ± 230 [d]	p_B = 1.7 ± 0.12% [d]		1600 ± 200 [d]	p_B = 7.6 ± 16% [d]	
Global fit (w/out I182, V186)	870 ± 130 [d]	p_B = 1.6 ± 0.15% [d]		1600 ± 220 [d]	p_B = 7.3 ± 18% [d]	

** [*methyl*-^{13}C] probes for activation loop residues I182 and V186

[a] Parameters were obtained from multiple quantum CPMG dispersion data collected at 25 °C.

[b] This term was estimated assuming a two-state exchange model under fast-exchange limit using 900 MHz CPMG dispersion data (Materials and Methods).

[c] R_{ex} was estimated using the equation $R_{ex} = R_{2,eff}(50\ \text{Hz}) - R_{2,eff}(1{,}000\ \text{Hz})$ from 900 MHz CPMG dispersion data.

[d] Parameters were obtained by fitting CPMG dispersion data collected at 900 MHz to a two-state exchange process using the Carver-Richards equation using the CATIA program.

Table S3B. Exchange parameters for [*methyl*-^{13}C]ILV probes in mutant V186I, 0P- and 2P-ERK2. [a]

Table S3B V186I	V186I 0P-ERK2			V186I 2P-ERK2		
	k_{ex} (s^{-1}) [b]	$p_A p_B \Delta\omega_{AB}^2$ (s^{-2}) [b]	R_{ex}(s^{-1}) [c]	k_{ex} (s^{-1}) [b]	$p_A p_B \Delta\omega_{AB}^2$ (s^{-2}) [b]	R_{ex}(s^{-1}) [c]
L67	3000 ± 1600	15000 ± 4900	4	ND [d]	ND	0
I70	2400 ± 540	12000 ± 1500	3	700 ± 340	9200 ± 1600	6
I72	2200 ± 300	27000 ± 2000	8	1300 ± 230	120000 ± 8300	54
L73	2000 ± 450	22000 ± 2600	7	650 ± 380	26000 ± 5600	15
L74	ND	ND	0	2200 ± 1400	21000 ± 7300	5
I81	1400 ± 500	7200 ± 1100	3	1500 ± 280	37000 ± 3100	16
I82	ND	ND	5	1800 ± 190	68000 ± 3400	28
I87	1700 ± 1000	64000 ± 1800	3	1500 ± 320	46000 ± 4300	22
I101	1800 ± 330	13000 ± 1100	4	1300 ± 78	39000 ± 970	20
I131	1600 ± 380	13000 ± 1400	5	1500 ± 880	34000 ± 8900	14
L135	2800 ± 920	35000 ± 7000	7	ND	ND	ND
I138	1100 ± 570	4800 ± 940	2	1900 ± 190	81000 ± 4000	31
V143	1200 ± 450	13000 ± 1900	3	1100 ± 840	24000 ± 6800	13
L148	3800 ± 3200	11000 ± 6100	2	1700 ± 980	30000 ± 8200	16
L154	3500 ± 1100	12000 ± 2500	3	ND	ND	2
L155	1500 ± 460	7800 ± 1100	2	1100 ± 160	37000 ± 2100	21
L182**	ND	ND	ND	ND	ND	ND
I186**	3300 ± 1200	55000 ± 12000	12	ND	ND	ND
I241	1800 ± 260	25000 ± 1800	10	1800 ± 160	94000 ± 4000	34
L288	ND	ND	0	1600 ± 430	33000 ± 4000	12
I345	ND	ND	0	2200 ± 230	55000 ± 3100	49
Global fit (w/out L182, I186)	No convergence[e]			1000 ± 110[f]	p_B = 6.9 ± 0.71%[f]	

** In these datasets [*methyl*-^{13}C] probes for activation loop residues L182 and I186 yielded signals that were too low to quantify reliably.

[a] Parameters were obtained from multiple quantum CPMG dispersion data collected at 25 °C.

[b] This term was estimated assuming a two-state exchange model under fast-exchange limit using 900 MHz CPMG dispersion data (Materials and Methods).

[c] R_{ex} was estimated using the equation $R_{ex} = R_{2,eff}(50\ \text{Hz}) - R_{2,eff}(1{,}000\ \text{Hz})$ from 900 MHz CPMG dispersion data.

[d] Individual fits and/or errors could not be determined.

[e] Global fitting attempts failed to converge.

[f] Parameters were obtained by fitting CPMG dispersion data collected at 800 and 900 MHz to a two-state exchange process using the Carver-Richards equation using the CATIA program.

Table S3 (cont.). Exchange parameters for [*methyl*-^{13}C]ILV probes in mutants L182I and V186I, 0P- and 2P-ERK2. [a]

Table S3C Jackknife analysis [a]	WT 2P-ERK2			
	k_{ex} (s^{-1}) [b]		p_B (%) [b]	
Trial 1: 15 residues (4 removed)	320	± 14	17	± 0.56
Trial 2: 9 residues (6 removed)	320	± 24	18	± 4.5
Trial 3: 10 residues (9 removed)	330	± 32	19	± 5.7
Averages:	320	± 23	18	± 3.6

Jackknife analysis	L182I 2P-ERK2			
	k_{ex} (s^{-1}) [b]		p_B (%) [b]	
Trial 1: 15 residues (4 removed)	1700	± 140	7.9	± 3.0
Trial 2: 9 residues (6 removed)	1600	± 210	7.8	± 3.6
Trial 3: 10 residues (9 removed)	1500	± 280	6.1	± 3.2
Averages:	1600	± 210	7.3	± 3.3

Jackknife analysis	L182I 0P-ERK2			
	k_{ex} (s^{-1}) [b]		p_B (%) [b]	
Trial 1: 15 residues (4 removed)	1000	± 370	7.0	± 16
Trial 2: 9 residues (6 removed)	1000	± 340	8.3	± 13
Trial 3: 10 residues (9 removed)	1000	± 470	14	± 22
Averages:	1000	± 390	9.8	± 17

Jackknife analysis	V186I 2P-ERK2			
	k_{ex} (s^{-1}) [b]		p_B (%) [b]	
Trial 1: 15 residues (4 removed)	1100	± 110	7.4	± 1.3
Trial 2: 9 residues (6 removed)	1100	± 180	8.0	± 1.9
Trial 3: 10 residues (9 removed)	960	± 280	8.4	± 3.4
Averages:	1100	± 190	7.9	± 2.2

[a] Parameters were obtained by fitting CPMG dispersion data collected at 900 MHz, 25 °C. Each trial involved 50 iterations in which 4, 6 or 9 residues were randomly removed from the set of 19 residues shown in Table S2A. For each iteration, the remaining residues were fit to a two-state exchange process using the Carver-Richards equation on a per-methyl basis.

[b] For each trial, reported values of k_{ex} and p_B represent averages and standard deviations over 50 iterations.